Synergistic effects on co-pyrolysis and co-combustion of sludge and coal investigated by thermogravimetric analysis

Hasan Merdun[1] · Zakari Boubacar Laougé[1] · Aslı Seyhan Çığgın[1]

Abstract

Thermal characteristics and kinetics of sewage sludge (SS), lignite coal, and their blends (25 and 50% of SS) in pyrolysis and combustion processes were investigated by using thermogravimetric analysis (TGA). TGA was carried out at different heating rates of 10, 20, and 40 K min^{-1} under inert and air atmospheres. Kinetics were calculated by Flynn–Wall–Ozawa, Starink, and Vyazovkin models by using TGA data. The deviation between the experimental and calculated values of mass loss, residual fraction, and activation energy was determined to highlight the synergistic effect between SS and coal. The results indicated that both mixtures influenced the initial and final temperatures of reactions. Mass loss of the mixtures during pyrolysis was not significantly influenced by the SS proportion, however, the residual fraction was influenced by the mixtures during pyrolysis and combustion. Blend of 50% SS with the smaller activation energy (Ea) compared to 25% SS was the most suitable for bioenergy production in pyrolysis, whereas in combustion 25% SS with small Ea was the most promising. On the other hand, 100% SS had the smallest Ea in both processes, indicating the optimum bioenergy source.

Keywords Sludge · Synergistic effects · Thermogravimetric analysis · Kinetic

Introduction

The increase in world's population, especially in urban areas, leads to the production of large quantities of municipal solids wastes (MSW) and wastewater. Wastewater causes pollution of surface and groundwater when it is discharged to the environment without treatment. Thus, wastewater treatment plants (WWTP) are available around the world, especially in developed countries. In recent years, worldwide production of sewage sludge (SS) from WWTP is increasing day by day in parallel to population, urbanization, and industrialization [1, 2]. In 2012, there were 460 WWTPs serving 58% of the population in Turkey. When the average SS production as 40–46 g of solid matter per capita per day for the served population was considered, approximately 1700–2600 tons of domestic or municipal SS per day was generated [3].

Sewage sludge is a common residue resulting from the treatment processes of industrial or municipal wastewaters [4] and a heterogeneous mixture made up of microorganisms, undigested organics, inorganic materials, and moisture (> 90%). It has been classified as biomass due to its high calorific value or semi-biomass in the literature [5]. SS is even sometimes compared to low-rank coals such as lignite in terms of energy content. However, it differs from plant biomass in many aspects such as high moisture and ash contents which might pose technical challenges to its thermochemical conversion [6]. SS can be a threat to the environment and human health because of the high the presence of heavy metals and pathogens if not properly treated [1, 2, 7–9].

Before disposal, SS is usually treated in order to reduce smell, the quantity of organic solids, water content, and eliminate some disease-causing bacteria. This treatment of reducing heavy metals and other harmful microorganisms can be made either anaerobically or aerobically. Approximately 50% of wastewater treatment cost is accounted for SS treatment and its treatment contributes to approximately 40% of greenhouse gas emissions released from wastewater treatment processes [3, 10]. The most used disposal methods of SS are direct landfill, dunghill for soil, and burning after being dehydrated [1]. However, co-utilization (co-pyrolysis or co-combustion) of SS with biomass or coal is currently used to convert dried SS into

✉ Hasan Merdun
merdun@alumni.clemson.edu

[1] Department of Environmental Engineering, Faculty of Engineering, Akdeniz University, 07058 Antalya, Turkey

higher-value fuels or chemicals. The specific benefits of co-utilization include the replacement of fossil fuels and the reduction of CO_2 emissions [9].

Several researches have been reported on co-pyrolysis/ co-combustion of sludge and coal/biomass. Co-pyrolysis characteristics study of Dianchi Lake sludge and coal was reported by Xia and Li [8], and the results showed that TG and DTG profiles of Dianchi Lake sludge were similar to coal, but different from coal under various blending ratios. Interaction was observed between the solid phases of Dianchi Lake sludge. Biagini et al. [11] investigated the devolatilization behavior of different coals and biomass under the heating rate of 20 °C min^{-1} and high nitrogen flowrate. Analysis of coal-biomass blends revealed that in the experimental conditions the mass loss of a blend could be gained from the sum of raw materials. Otero et al. [12] reported that the dried SS could be co-fired at a percentage of up to 50% with no major consequences regarding gaseous emissions. An investigation by Folgueras et al. [13] using thermogravimetric analysis (TGA) of SS and bituminous coal blends revealed that blends with a SS content of 10% behaved similarly to coal, whereas blends of 50% clearly showed two combustion stages (a clear volatile matter and more reactive structures stage and a second thermal decomposition stage of more complex structures). Ninomiya et al. [14] showed that SS combustion with coal had better performance than SS mono-combustion. Chen et al. [15] investigated the interactions between wastewater solid and lignite in the process of co-combustion under different blending ratios. The results showed that the comprehensive combustion performance of the blends increased as the mass percentage of wastewater solid in the blends increased. Co-utilization (co-pyrolysis or co-combustion) of SS and coal instead of individually using them may have benefits like synergistic effects of SS with higher energy efficiency and better evaluation of low-quality coal. Unlike previous studies, such a comprehensive study on co-utilization of SS and coal in different processes (pyrolysis and combustion) with different blend ratios and kinetic models, and synergy analysis may help to design optimum process conditions.

Therefore, the present study aimed to investigate the thermal decomposition of SS and coal by pyrolysis and combustion as well as the synergistic effect during co-pyrolysis and co-combustion in two different blend ratios using TGA. The blend 25SS referred to 25% SS + 75% coal, while 50SS referred to 50% SS and 50% coal. Kinetic parameters were calculated by using three different kinetic models namely Flynn–Wall–Ozawa (FWO), Starink, and Vyazovkin. To highlight the synergistic effect, the deviation between the experimental and calculated values was determined.

Materials and methods

Materials

SS used in this study was collected from the WWTP of Hurma, Antalya, Turkey. Raw SS was left for drying in stove at 60°K in the Environmental Engineering Department Laboratory of Akdeniz University. The dried SS was milled and sieved to get the desired particle size of 180–212 μm for its characterization and TGA. Lignite coal was collected from Elbistan coal basin located in Karahmanmaras, Turkey. Coal was once crumbled to small pieces and then left for air drying. The dried coal was then milled and sieved to fine particles suitable for characterization and TGA experiments.

Feedstock characterization and TGA

Proximate analysis of SS and coal was carried out in order to determine its moisture, ash, and volatile matter contents according to ASTM standards at the Environmental Engineering Department Laboratory of Akdeniz University. Ultimate analysis for samples was performed using LECO analyzer at the Scientific and Technological Research Laboratory of Inönü University. Carbon (C), hydrogen (H), nitrogen (N), and sulfur (S) contents were detected directly, while oxygen (O) content was calculated by difference. Higher heating value (HHV) was calculated by using the results of ultimate analysis. Components analysis of SS was also conducted in order to determine its cellulose, hemicellulose, lignin, and extractives contents.

TGA experiments were performed from the room temperature to 1000 °C under three different heating rates (β) of 10, 20, and 40 K min^{-1} by using nitrogen and air of 100 mL min^{-1}. About 10 mg of sample was used in Pyris Series STA-8000 (Perkin Elmer Co., Ltd, USA) thermogravimetric analyzer at the Material Science and Engineering Laboratory of Akdeniz University. Each experiment was repeated at least three times for repeatability. Data from TGA were used to determine kinetic parameters.

Synergistic effect

In order to highlight the synergistic effect between SS and coal, the difference between the experimental and calculated (named deviation) mass loss and residual fraction of the mixtures was determined [16].

$$\text{Deviation} = \frac{\text{Exp}_{\text{value}} - \text{Cal}_{\text{value}}}{\text{Cal}_{\text{value}}} \times 100, \tag{1}$$

where $\text{Exp}_{\text{value}}$ is the value obtained from the curve of mixture, $\text{Cal}_{\text{value}}$ is the value calculated as the sum of the TGA curves of individual samples according to the ratio as expressed in Eq. (2):

$$\text{Cal}_{\text{value}} = \left(\text{Exp}_{\text{SS}} \times \lambda_{\text{SS}}\right) + \left(\text{Exp}_{\text{coal}} \times \lambda_{\text{coal}}\right), \tag{2}$$

where Exp_{SS} and Exp_{coal} are the experimental values of SS and coal, λ_{SS} and λ_{coal} are the proportions of SS and coal in the mixture. Activation energy (Ea) deviation was calculated as follows:

$$\text{Deviation} = E_{\text{exp}} - E_{\text{cal}}, \tag{3}$$

where E_{exp} and E_{cal} are the experimental and calculated Ea values.

Kinetic

Ea as a kinetic parameter can be determined using kinetic analysis equations derived from a combination of the basic rate equation and the Arrhenius equation. Kinetic equation for the thermal decomposition reactions of solid-state matter is expressed based on mass conversion rate (α) as in Eq. (4):

$$\frac{d\alpha}{dt} = k(T)f(\alpha), \tag{4}$$

where α is the degree of mass conversion during thermal decomposition, $d\alpha/dt$ stands for the rate of conversion, t is time, T is the absolute temperature, $k(T)$ is temperature-dependent rate constant, and $f(\alpha)$ is the function of reaction mechanism. Then, α can be expressed as in Eq. (5):

$$\alpha = \left(\frac{m_0 - m_{\text{t}}}{m_0 - m_{\text{f}}}\right), \tag{5}$$

where m_0 is the initial mass of the sample, m_{t} is the mass of the sample at time t, and m_{f} is the final mass of the sample at the end of the reaction. According to the Arrhenius law $k(T)$ is the reaction rate constant that may be expressed as in Eq. (6):

$$k(T) = A \exp\left(-\frac{\text{Ea}}{\text{RT}}\right), \tag{6}$$

where Ea (kJ mol^{-1}) is the activation energy of reaction, A is the pre-exponential or frequency factor, R is the universal gas constant. Equations (4) and (6) can be combined to give:

$$\frac{d\alpha}{dt} = A \exp\left(-\frac{\text{Ea}}{\text{RT}}\right)f(\alpha) \tag{7}$$

If the temperature increases with the constant heating rate (β, K min^{-1}), then

$$\beta = \frac{dT}{dt} = \frac{dt}{d\alpha} = \frac{d\alpha}{dt}$$

dt can be introduced to transform Eq. (8) as follows:

$$\frac{d\alpha}{dT} = \frac{A}{\beta} \exp\left(-\frac{\text{Ea}}{\text{RT}}\right)f(\alpha) \tag{8}$$

The integration function of Eq. (8) is expressed as Eq. (9). Therefore, Eq. (9) is the fundamental equation that preamble the determination of non-isothermal solid-state thermal degradation kinetic methods to determine the kinetic mechanisms parameters.

$$\int_0^\alpha \frac{d\alpha}{f(\alpha)} = g(\alpha) = \frac{A}{\beta} \int_{T0}^T \exp-\left(\frac{E}{RT}\right)dT \tag{9}$$

and T is defined as follows:

$$T = T_0 + \beta t, \tag{10}$$

where $g(\alpha)$ is the integral function of conversion and T_0 (K) is the initial temperature of the experiment.

Kinetic parameters of a considered process can be analyzed by using different isoconversional and non-isoconversional methods. Isoconversional methods provide straight lines consisting of points at different β values for each α and therefore allow the determination of kinetic parameters at different α values. In isoconversional methods, α for a reaction is assumed to be constant such that the rate of reaction depends absolutely on the reaction temperature (T). In this study, three different isoconversional models were used to determine Ea of different samples.

FWO model

FWO model is an isoconversional linear integral model based on Doyle's approximation which allows Ea to be obtained from the plot of natural logarithm of heating rates ($\ln\beta$) versus (1/T) [17–19] as:

$$\ln(\beta) = \ln\left(\frac{A\,\text{Ea}}{R\,g(\alpha)}\right) - 5.331 - 1.052\frac{\text{Ea}}{\text{RT}}, \tag{11}$$

where α is the mass loss ratio of the sample, t is the time, $\beta = dT/dt$ is the heating rate, T is the reaction temperature or absolute temperature corresponding to the value of α, A is the pre-exponential factor as Arrhenius parameters, Ea is the apparent activation energy as a function of α, R is the universal gas constant, and $g(\alpha)$ is the integral form of kinetic model which is constant at a given value of α. Ea can be determined from the slope ($-1.052\text{Ea}/R$) of the straight line obtained from the plot of $\ln(\beta)$ versus (1/T).

Vyazovkin model

Vyazovkin model [20, 21] determines Ea by the slope $(-E_\alpha/R)$ of the straight line obtained from the plot of $\ln(\beta/T_\alpha^2)$ versus $(T)^{-1}$ by using the following equation:

$$\ln\left(\frac{\beta}{T_\alpha^2}\right) = \ln\left(\frac{AR}{Eag(\alpha)}\right) - \frac{Ea}{RT_\alpha}, \tag{12}$$

where β is the heating rate (K min^{-1}). Ea is obtained as a function of α. For each α value, the plot of $\ln(\beta/T_\alpha^2)$ versus $(1/T)$ gives a straight line with slope $(-Ea/R)$.

Starink model

Starink model was based on OFW and KAS models and made a further accurate analysis of the temperature integral [22]:

$$\ln\left(\frac{\beta}{T_\alpha^S}\right) = \frac{BEa}{RT_\alpha} + C_S, \tag{13}$$

where β is the heating rate (K min^{-1}), S, B, and C_s are constant. After the temperature integral was further accurate analyzed, the equation above could be converted into the following equation:

$$\ln\left(\frac{\beta}{T_\alpha^{1.8}}\right) = -1.0037\frac{Ea}{RT_\alpha} + C_S \tag{14}$$

For α = constant, Ea could be obtained by the slope of the straight line by plotting $\ln(\beta/T_\alpha^{1.8})$ versus $1/T_\alpha$.

Results and discussion

Feedstock characterization

Proximate, elementary, and structural analyses of SS and coal are given in Table 1. It can be seen that coal had higher moisture content (13.77%) than SS (5.42%). Moisture content of SS was comparable with the literature [2]. As expected, SS had higher volatile matter content (65.48%) than coal (37.57%). Moreover, in this study, coal had higher fixed carbon content (23.58%) compared to SS (9.27%). Volatile matter and fixed carbon contents of SS were comparable to those reported by He et al. [16]. Ash content was higher in coal than SS as opposed to the literature [1, 2]. Elementary analysis showed that C content was high in SS (42.73%) and exceeded the results (30–40%) reported by Otero et al. [12]. C content of coal found as 28.12% was less than the reported by Otero et al. [12] as 74%. H content of SS in this study (6.08%) was comparable to those reported

Table 1 Main characteristics of feedstock

	Sludge	coal
Proximate analysis		
Moisture/%	5.42	13.77
Volatile matter/%	65.48	37.57
Fixed carbon/%	9.27	23.58
Ash/%	19.84	25.07
Ultimate analysis		
C/%	42.73	28.12
H/%	6.08	3.42
O/%[a]	45.29	66.45
N/%	5.26	0.75
S/%	0.64	1.26
H/C	0.14	0.12
O/C	1.06	2.36
HHV/MJ kg^{-1}	16.96	6.44
Components analysis		
Cellulose/%	31.32	
Hemicellulose/%	14.48	
Holocellulose	45.80	
Lignin/%	24.65	
Extractives/%	28.98	

[a]Calculated by difference

by Chen et al. [1] and He et al. [16] as 5.29 and 6.20%, respectively. Coal had higher O content (66.45%) compared to SS (45.29%). This result agreed with the literature, indicating that high O content of coal limits its use. As expected, SS has higher N content (5.26%) compared to coal (0.75%). This high N content appears from protein fraction of microorganisms used in WWTP [23]. S content of coal (1.26%) was much higher than that of SS (0.64%). In general, SS has high N and S contents compared to biomass as reported by Naqvi et al. [23]. Since N and S are present in feedstocks as the major sources of emission, combustion of mixture requires more interest to avoid pollution issues. Lignite coal known as a low-rank coal had lower HHV (6.44 MJ kg^{-1}) than SS (16.96 MJ kg^{-1}) which was comparable with the literature [16] and higher than those reported by Chen et al. [1] and Niu et al. [2]. Components analysis results of SS used in this study had some similarities to lignocellulosic biomass [6].

Pyrolysis

Pure SS and coal

Figure 1 shows TG and DTG curves of different samples under pyrolysis (N$_2$) and combustion (Air). Temperatures and mass losses from DTG are summarized in Table 2. Thermal degradation of both materials (SS and coal) can
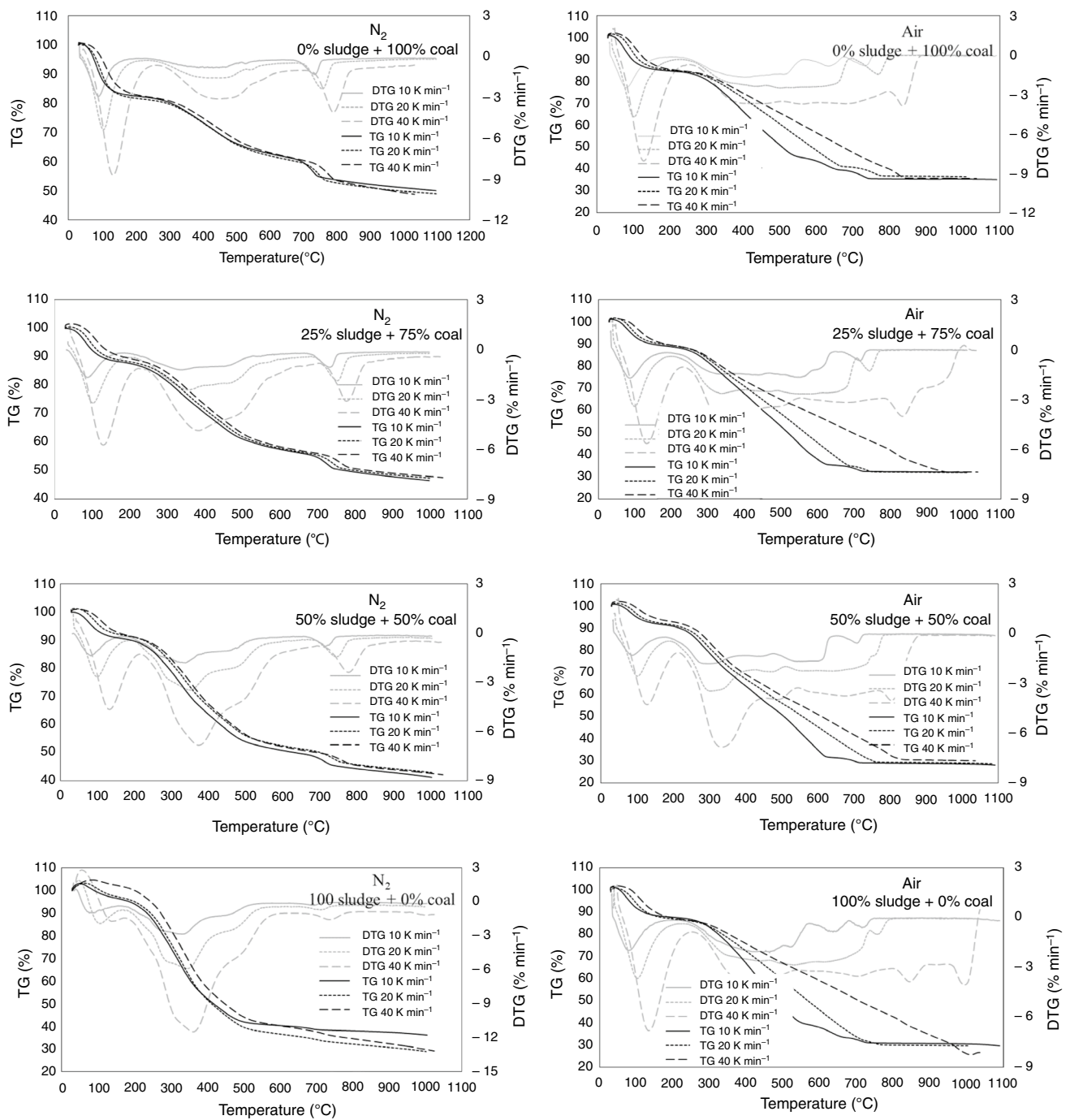
Fig. 1 TG and DTG curves of co-pyrolysis and co-combustion of sludge and coal at different blend ratios and heating rates

be subdivided into three phases: vaporization of moisture and other impurities, volatilization of volatile matters, and degradation of non-biodegradable organic matter [24] and inorganic contents such as calcium carbonate [23]. The first phase taking place from the room temperature to 190 and 250 K for SS and coal, respectively, showed similar peaks. For example, for β of 20 K min^{-1}, peaks were 106.87 and 103.52 °C for SS and coal, respectively. During this phase, mass loss of coal was higher with an average of 17.72% against 2.51% for SS. The second phase considered as the main phase of reaction showed peaks for β of 10, 20, and 40 K min^{-1} at 331.27, 350.95, and 366.55 K; and 462.76, 476.49, and 479.21 K for SS and coal, respectively. This trend showed that peak temperature was a function of β,

Table 2 Characteristics temperatures associated with the mass losses in different stages of decomposition during co-pyrolysis and co-combustion of sludge and coal at different blend ratios and heating rates

Process blend ratio	β/ K min^{-1}	T_{min}/K	ML-I/%	T_1/K	ML-II/%	T_2/K	ML-III/%	T_{max}/K	FR/%
N_2 0% sludge + 100% coal	10	30	17.03	170	28.67	770	4.32	1098	49.98
	20		18.11	190	29.18	800	3.96	1099	48.95
	40		18.01	250	29.50	840	3.72	1034	48.77
N_2 25% sludge + 75% coal	10	30	11.68	170	28.52	530	13.38	998	46.42
	20		11.50	190	28.97	550	12.24	1000	47.29
	40		11.50	230	30.53	615	10.49	1034	47.48
N_2 50% sludge + 50% coal	10	30	9.49	170	37.86	530	11.53	1003	41.12
	20		8.95	200	37.24	550	11.00	1004	42.81
	40		9.83	225	37.83	590	10.28	1034	42.06
N_2 100% sludge + 0% coal	10	30	3.88	165	54.38	510	5.47	1005	36.27
	20		3.65	180	58.56	550	8.85	1002	28.94
	40		0.00	190	58.89	570	11.92	1025	29.19
Air 0% sludge + 100% coal	10	30	15.11	190	49.36	750	0.45	1092	35.08
	20		15.15	220	48.14	810	0.29	1008	36.42
	40		15.53	250	48.74	890	0.15	1037	35.58
Air 25% sludge + 75% coal	10	30	10.60	170	59.96	730	0.45	1006	31.99
	20		10.41	195	57.42	780	0.29	1008	31.88
	40		11.68	240	53.31	890	2.88	1037	32.13
Air 50% sludge + 50% coal	10	30	8.31	170	62.56	740	0.98	1091	28.15
	20		8.25	190	62.33	780	0.71	1083	28.71
	40		7.80	220	61.82	890	0.35	1036	30.03
Air 100% sludge + 0% coal	10	30	11.92	180	57.17	750	1.29	1090	29.62
	20		13.14	210	56.87	790	0.38	1008	29.61
	40		13.88	255	50.11	880	9.39	1037	26.62

β: heating rate; ML: mass losses at the decomposition stages I, II, and III; FR: final residues

where when β increased peak temperature also increased. This trend was the same for the initial and final temperatures as reported by Otero et al. [25]. The average mass loss of SS (57.27%), proportional to its volatile matter content, was greater than that of coal (29.12%). It should be noted that mass loss for a given sample did not change significantly as a function of β. The third phase related to the degradation of complex molecules and biochar formation took place at high temperature for SS and coal. This trend highlights the presence of complex molecules in SS and coal. As expected, for β of 10, 20, and 40 K min^{-1} peak temperatures of coal were 748.29, 760.34, and 792.10 K, respectively, which were higher than that of SS as 706.56, 725.38, and 748.37 K. In this phase the average mass loss of 4 and 8.75% for coal and SS, respectively remains very insignificant. Coal with a high fixed carbon compared to SS showed an average residual fraction of 49.23% greater than that of SS (31.47%). Due to the relatively high fixed carbon contents of SS and coal as well as the residual fraction in pyrolysis, it can be affirmed that SS and coal can be used in biochar production.

Blends (25SS and 50SS)

As for the individual samples, the representative curves of 25SS and 50SS can also be subdivided into three phases. These phases, which were often sharper than for the individual samples, were the result of interactions between SS and coal. To evaluate the synergistic effect between SS and coal, the difference between the experimental and calculated values of the different mixtures was determined as tabulated in Table 3. The observation of curves allowed us to note the exitance of three different peaks. TG curves were very close to each other when β increased as reported by Hamnin et al. [7]. The evaporation phase for β of 10, 20, and 40 K min^{-1} of 25SS had peaks at 84.66, 104.74, and 132.42 K, respectively, and 82.65, 100.54, and 136.30 K for 50SS. These peak temperatures followed the same trend as that of the individual SS and coal for the same phase. The average mass loss during this phase was 11.56 and 9.42% for 25SS and 50SS, respectively. In general, for a given phase the variation of mass loss was negligible as a function of β. The second phase had temperature peaks oscillating between the peak temperatures of SS and coal in DTG curves. Thus, the peak

Table 3 Deviation between the experimental and calculated values during pyrolysis and combustion of 25SS and 50SS at different heating rates

Process blend ratio	β/K min^{-1}	T_1/K	T_2/K	ML$_{max}$/%	FR/%	ML	FR	Volatile	Char	Ash
N$_2$ 0% sludge + 100% coal	10	170	770	28.67	49.98	NA	NA	NA	NA	NA
	20	190	800	29.18	48.95	NA	NA	NA	NA	NA
	40	250	840	29.50	48.77	NA	NA	NA	NA	NA
N$_2$ 100% sludge + 0% coal	10	165	510	54.38	36.27	NA	NA	NA	NA	NA
	20	180	550	58.56	28.94	NA	NA	NA	NA	NA
	40	190	570	58.89	29.19	NA	NA	NA	NA	NA
N$_2$ 25% sludge + 75% coal	10	170	530	28.52	46.42	35.10	46.55	− 18.75	− 0.28	
	20	190	550	28.97	47.29	36.53	43.95	− 20.70	7.60	
	40	230	615	30.53	47.48	36.85	43.88	− 17.15	8.20	
N$_2$ 50% sludge + 50% coal	10	170	530	37.86	41.12	41.53	43.13	− 8.84	− 4.66	
	20	200	550	37.24	42.81	43.87	38.95	− 15.11	9.91	
	40	225	590	37.83	42.06	44.20	38.98	− 14.41	7.90	
Air 0% sludge + 100% coal	10	190	750	49.36	35.08	NA	NA	NA	NA	
	20	220	810	48.14	36.42	NA	NA	NA	NA	
	40	250	890	48.74	35.58	NA	NA	NA	NA	
Air 100% sludge + 0% coal	10	180	750	57.17	29.62	NA	NA	NA	NA	
	20	210	790	56.87	29.61	NA	NA	NA	NA	
	40	255	880	50.11	26.62	NA	NA	NA	NA	
Air 25% sludge + 75% coal	10	170	730	59.96	31.99	51.31	33.72	16.86		− 5.13
	20	195	780	57.42	31.88	50.32	34.72	14.11		− 8.18
	40	240	890	53.31	32.13	49.08	33.34	8.62		− 3.63
Air 50% sludge + 50% coal	10	170	740	62.56	28.15	53.27	32.35	17.44		− 12.98
	20	190	780	62.33	28.71	52.51	33.02	18.70		− 13.05
	40	220	890	61.82	30.03	49.43	31.10	25.07		− 3.44

temperatures of 25SS and 50SS were higher than the peak temperature of SS and lower than that of coal. However, the peak temperatures of 25SS and 50SS for β of 10, 20, and 40 K min^{-1} were 353.28, 366.37, and 375.38 K; and 353.39, 358.26, and 378.67 K, respectively; where the peaks were similar and present very little variation. The increase or shift in temperature is related to the rates of heat and mass transfer taking place because of increasing the heat input to the system. Under the heat and mass transfer conditions, the time of transfer and size of sample influence the reaction rate and possibly the mechanism. Therefore, it could easily be said that the mixture of SS and coal had an effect on the initial and final temperatures of reactions. For this phase, the average mass loss was 29.34 and 37.64% for 25SS and 50SS, respectively. The third phase followed the same trend as the previous phases from the peak temperature point of view. Average mass loss during this phase was found as 12.03 and 10.93% for 25SS and 50SS, respectively. This highlights the formation of complex molecules during the reactions of 25SS and 50SS. These molecules difficult to degrade need higher reaction temperature.

To better perceive the synergistic effect, the experimental and calculated values of mass loss and residual fraction were compared. For 25SS it was found that the calculated values

of mass loss were greater than the experimental values, where the negative difference indicates a lack of synergy. Indeed, the proportion of coal greater than that of SS, large amount of volatile matter contained in SS had too little effect on the volatiles of 25SS. The experimental values of mass loss of 25SS were close to that of coal. This situation was almost the same for 50SS. However, the experimental mass loss, although closer to that of coal, increased considerably. With regard to the remained residues named as biochar or residual fraction in pyrolysis, it was found that apart from β of 10 K min^{-1}, all other differences were positive. This situation describes the presence of a synergy between SS and coal during biochar formation. For 25SS, the experimental values were closer than that of coal, whereas for 50SS the experimental values oscillated between the values of SS and coal. Therefore, it can be conclude that 25SS and 50SS are favorable for biochar production.

As expected, the curves of α as a function of temperature followed the same trend for all samples (Fig. 2). Indeed, α increased with temperature for all samples regardless of β. However, for the same α temperature of reaction increased with β. It was also observed that for pure coal reaction extended to above 1000 °C, whereas for SS the majority of reaction ended between 700 and
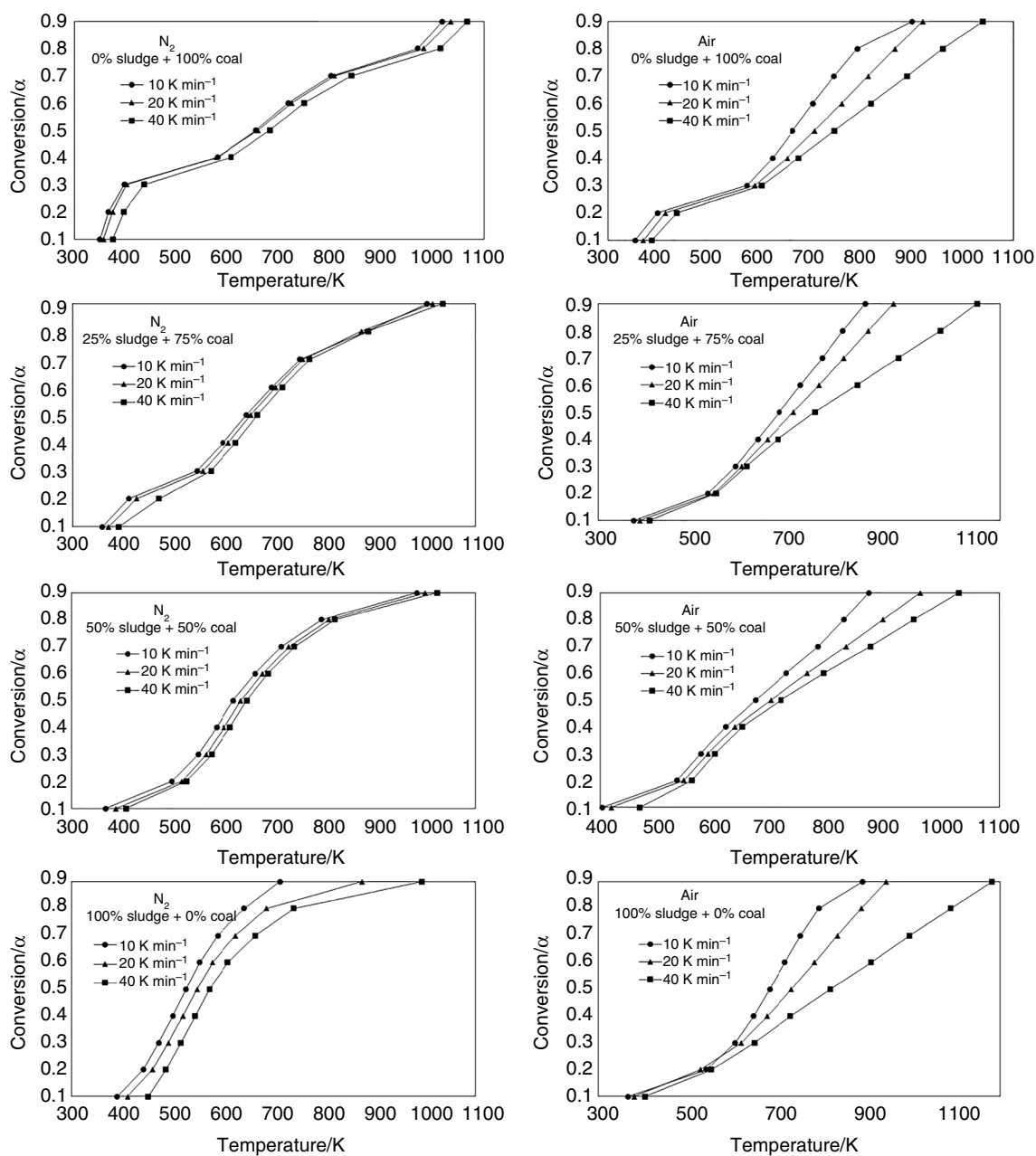
Fig. 2 Relationship between mass conversion point and temperature for co-pyrolysis and co-combustion of sludge and coal at different blend ratios and heating rates

800 K. For 25SS, 70% of the reactions ended at 752.20, 758.05, and 771.45 °C for β of 10, 20, and 40 K min^{-1}, respectively. Finally, for 50SS 80% of the reactions took place between 0.1 and 0.8 of α, where temperatures were 367.00, 387.84, and 407.25 K; and 795.89, 810.25, and 821.96 K for β of 10, 20, and 40 K min^{-1}, respectively.

Combustion

Pure SS and coal

TG and DTG curves of SS and coal during combustion can also be subdivided into three phases. The first phase corresponding to the volatilization of water in the samples took place from the ambient temperature to 255 and 250 K for SS and coal, respectively. Mass loss during this phase was

almost constant for coal and varies very little for SS depending on β of 10, 20, and 40 K min^{-1}. In general, for all samples, mass loss for a given sample varied very little according to β. The second phase representing the most important part of reaction for SS and coal had peak temperatures at 526.14, 531.30, and 536.46 K; and 522.13, 557.37, and 577.57 K and the rate of mass loss (dw/dt) of -1.71, -2.84, and -3.15% min^{-1}; and -1.35, -2.43, and -3.67% min^{-1} for β of 10, 20, and 40 K min^{-1}, respectively. The average peak temperatures of SS were lower than that of coal, but the average dw/dt was opposite. This may be due to the high amount of volatile of SS. It was found that peak temperatures as well as dw/dt were a function of β for all samples. The third phase corresponding to the decomposition of char and the formation of ash continued above 1000 K. During this phase, mass loss was generally insignificant for all samples except SS and 25SS for β of 40 K min^{-1}. The residual fraction consisting essentially of ash was found as 28.62 and 35.93% for SS and coal, respectively. It can be seen that although SS has a high ash content [1], its combustion produces less ash than coal. Ash is an undesirable matter in the configuration of combustion reactors. Thus, less ash release feedstock is, the more desirable it is for combustion.

Blends (25SS and 50SS)

Like pure SS and coal, three phases were also observed in 25SS and 50SS. Moisture release for 25SS and 50SS occurred at peak temperatures of 86.85, 102.34, and 135.90 K; and 82.17, 103.83, and 129.95 K for dw/dt of -1.71, -3.39, and -5.63% min^{-1}; and -1.27, -2.54, and -4.26% min^{-1} for β of 10, 20, and 40 K min^{-1}, respectively. It can be said that dw/dt was a function of β and increased with β. The second phase taking place between 240 and 890 K for 25SS, and 220 and 890 K for 50SS corresponded to the degradation of volatile matters. The initial temperature of blended fuels decreased when SS proportion in blend increased as reported by Zhang et al. [26]. During this phase, the average mass losses of 25SS and 50SS were 56.89 and 62.30%, respectively. The average residual fraction in the third phase, where mass loss was almost zero, was 32 and 28.96% for 25SS and 50SS, respectively. For 25SS and 50SS, it was found that the residual fractions did not change significantly. However, 50SS producing less ash seems to be more suitable for combustion compared to 25SS.

To demonstrate the synergistic effect between SS and coal, the experimental and calculated values of mass loss and the residual fraction (ash) were compared. For both mixtures, there was a synergistic effect on mass loss. Indeed, for both cases, the positive deviation showed that high volatile matter content of SS played an important role in the reaction of mixture during co-combustion. When the proportion of SS in the mixture increased from 25 to 50%, the average

mass loss also increased from 56.89 to 62.24%. Since ash is undesirable in combustion, the negative deviation observed at the residual fraction was good for the reaction. However, the residual fraction of 25SS was closer to that of coal than that of SS, whereas it was opposite for 50SS. According to the results, the proportion of SS in the mixture influences the residual fraction in both processes; however, it did not have effect on the mass loss. As expected, α was a function of temperature which was a function of β (Fig. 2). Indeed, when β increased temperature also increased for the same α. For example, for coal, when $\alpha = 0.1$, temperature of the reaction was 352.95, 369.54, and 385.53 °C for β of 10, 20, and 40 K min^{-1}, respectively. For the same β value α, increased with temperature. For example, on SS curve for β of 40 K min^{-1}, when α increased from 0.1 to 0.2, temperature also increased from 404.17 to 552.41 K. This situation was almost identical for all samples. For combustion in general, most of the reaction took place above 500 K for all samples. For SS, 25SS, and 50SS only 10% of the reaction took place before 500 K and 20% for coal.

Kinetic analysis

Pyrolysis kinetic

Kinetic data are of major interest in the technological development for energy production through pyrolysis and combustion [24]. Three different models such as FWO, Starink, and Vyazovkin were used to calculate Ea of SS, coal, and their blends. The regression equations of all models are given in Table 4. Ea describes the energy barriers of chemical reactions and plays an important role in kinetic analysis [27]. From a general point of view, Ea varied according to α for all samples (Fig. 3). However, the variation was different from sample to sample. For coal, Ea as a function of α decreased between 0.1 and 0.3 then increases from 0.4 to 0.9 except 0.7. The variation of Ea was not similar at different α values because solid-state reaction was not simple one-step mechanism and occur in complex multistep reactions [28]. Average Ea calculated by FWO, Starink, and Vyazovkin were 133.99, 130.47, and 129.84 kJ mol^{-1}, respectively. The variation of Ea from 0.1 to 0.3 was almost constant for Starink and Vyazovkin models and showed little difference from that of FWO. In general, Ea values calculated by Starink and Vyazovkin models were very close to each other. This variation of Ea showed that the degradation of molecules contained in coal took place at different temperatures. Thus, the first three α values corresponded to the vaporization of moisture and degradation of certain volatiles. As temperature increased, the degradation of more complex molecules was realized. For SS Ea increased for α from 0.1 to 0.5 and then decreased regardless of the model used. It was noted that the degradation of complex molecules requiring maximum of Ea

Table 4 Activation energies at different mass conversion points calculated by different kinetic models for co-combustion of sludge and coal at different blend ratios and heating rates

Blending model	α	0% sludge + 100% coal			25% sludge + 75% coal			50% sludge + 50% coal			100% sludge + 0% coal		
		E/kJ mol^{-1}	$y=$	R^2	/kJ mol^{-1}	$y=$	R^2	/kJ mol^{-1}	$y=$	R^2	E/kJ mol^{-1}	$y=$	R^2
FWO	0.1	54.37	$-6879.8x+22.103$	0.95	46.33	$-5862.8x+18.69$	0.99	40.58	$-5134.7x+16.275$	1.00	50.80	$-6427.3x+15.799$	0.98
	0.2	50.09	$-6338.6x+19.74$	0.94	33.47	$-4235.1x+12.737$	0.95	95.39	$-12070x+26.449$	0.94	82.94	$-10494x+22.359$	0.99
	0.3	41.06	$-5195.1x+15.646$	0.84	121.27	$-15345x+30.407$	0.99	129.73	$-16416x+32.075$	0.99	92.45	$-11698x+23.569$	1.00
	0.4	101.07	$-12789x+24.769$	0.68	163.61	$-20703x+36.904$	0.99	146.73	$-18566x+33.89$	0.99	99.45	$-12583x+24.196$	1.00
	0.5	156.34	$-19783x+32.717$	0.88	205.95	$-26060x+42.74$	0.99	160.95	$-20365x+35.083$	0.99	102.67	$-12992x+24.034$	1.00
	0.6	173.94	$-22009x+33.109$	0.91	262.73	$-33244x+50.106$	0.98	189.94	$-24034x+38.449$	0.99	91.57	$-11586x+20.958$	1.00
	0.7	162.68	$-20584x+28.194$	0.88	314.98	$-39856x+55.405$	0.95	220.52	$-27904x+41.239$	0.99	77.83	$-9848.1x+17.377$	1.00
	0.8	230.82	$-29206x+32.531$	0.94	91.59	$-11589x+16.131$	0.02	273.66	$-34628x+45.787$	1.00	70.14	$-8875x+14.992$	1.00
	0.9	235.49	$-29798x+31.65$	0.97	359.54	$-45494x+47.688$	0.97	275.69	$-34884x+37.778$	1.00	33.29	$-4212.5x+7.7848$	0.97
	Mean	133.99		0.89	177.72		0.87	170.36		0.99	77.90		0.99
Starink	0.1	51.58	$-6227.3x+9.6953$	0.94	42.97	$-5187.2x+6.2195$	0.99	36.78	$-4439.6x+3.7524$	1.00	45.69	$-5516.5x+2.7896$	0.97
	0.2	46.81	$-5651.6x+7.2386$	0.93	28.50	$-3441.2x-0.0265$	0.92	92.35	$-11148x+13.42$	0.93	78.82	$-9515.7x+9.2208$	0.99
	0.3	36.82	$-4445.2x+2.9864$	0.79	118.74	$-14335x+17.213$	0.99	127.58	$-15402x+18.874$	0.99	88.40	$-10673x+10.346$	1.00
	0.4	97.11	$-11724x+11.479$	0.64	162.37	$-19602x+23.555$	0.99	144.84	$-17486x+20.575$	0.99	95.37	$-11514x+10.898$	1.00
	0.5	153.88	$-18578x+19.205$	0.86	206.07	$-24878x+29.263$	0.99	159.24	$-19225x+21.67$	0.99	98.40	$-11879x+10.665$	1.00
	0.6	171.36	$-20687x+19.43$	0.90	264.83	$-31972x+36.497$	0.98	188.99	$-22816x+24.918$	0.99	86.34	$-10423x+7.51$	1.00
	0.7	158.24	$-19104x+14.311$	0.86	318.78	$-38484x+41.659$	0.95	220.27	$-26592x+27.575$	0.99	71.36	$-8614.6x+3.8216$	1.00
	0.8	227.11	$-27418x+18.308$	0.93	82.87	$-10004x+2.1266$	0.02	274.78	$-33172x+31.935$	1.00	62.46	$-7540.4x+1.2948$	1.00
	0.9	231.26	$-27919x+17.339$	0.96	361.63	$-43658x+33.418$	0.96	273.99	$-33077x+23.536$	0.99	21.95	$-2649.6xx-6.2071$	0.95
	Mean	130.47		0.87	176.31		0.87	168.76		0.99	72.09		0.99
Vyazovkin	0.1	51.17	$-6154.8x+8.3166$	0.94	42.50	$-5112.2x+4.8338$	0.98	36.27	$-4362.4x+2.361$	1.00	45.02	$-5415.3x+1.3441$	0.96
	0.2	46.35	$-5575.3x+5.8495$	0.93	27.88	$-3352.9x-1.4447$	0.91	91.84	$-11046x+11.972$	0.93	78.21	$-9407x+7.761$	0.99
	0.3	36.26	$-4361.9x+1.5798$	0.79	118.25	$-14223x+15.747$	0.99	127.11	$-15289x+17.407$	0.99	87.78	$-10559x+8.8773$	1.00
	0.4	96.49	$-11605x+10.002$	0.64	161.96	$-19480x+22.072$	0.99	144.38	$-17366x+19.095$	0.99	94.74	$-11395x+9.4207$	1.00
	0.5	153.34	$-18444x+17.704$	0.86	205.74	$-24747x+27.766$	0.99	158.78	$-19098x+20.179$	0.99	97.73	$-11755x+9.18$	1.00
	0.6	170.77	$-20540x+17.91$	0.90	264.64	$-31831x+34.984$	0.98	188.57	$-22681x+23.414$	0.99	85.59	$-10294x+6.0157$	1.00
	0.7	157.46	$-18939x+12.769$	0.86	318.69	$-38332x+40.132$	0.95	219.87	$-26446x+26.056$	0.99	70.48	$-8477.5x+2.3155$	1.00
	0.8	226.30	$-27219x+16.728$	0.93	81.71	$-9828.2x+0.5705$	0.02	274.45	$-33010x+30.396$	1.00	61.46	$-7392.1x-02,272$	1.00
	0.9	230.38	$-27710x+15.749$	0.96	361.27	$-43454x+31.832$	0.97	273.33	$-32876x+21.954$	0.99	20.59	$-2475.9x-7.7617$	0.94
	Mean	129.84		0.87	175.85		0.87	168.29		0.99	71.29		0.99

Table 4 (continued)

Blending model	α	0% sludge + 100% coal			25% sludge + 75% coal			50% sludge + 50% coal			100% sludge + 0% coal		
		E/kJ mol⁻¹	$y=$	R^2	/kJ mol⁻¹	$y=$	R^2	/kJ mol⁻¹	$y=$	R^2	E/kJ mol⁻¹	$y=$	R^2
FWO	0.1	45.70	$-5782.4x+18.672$	1.00	50.81	$-6429.3x+19.506$	0.99	29.62	$-3748.1x+11.733$	0.93	42.45	$-5370.9x+17.021$	0.98
	0.2	48.21	$-6099.9x+17.717$	0.99	170.17	$-21533x+42.774$	0.91	128.08	$-16207x+32.653$	1.00	56.60	$-7162.1x+16.251$	0.19
	0.3	129.52	$-16388x+30.831$	1.00	167.50	$-21195x+38.223$	0.99	148.66	$-18811x+34.973$	1.00	95.08	$-12031x+22.272$	0.96
	0.4	88.18	$-11158x+20.146$	0.99	109.84	$-13898x+24.131$	1.00	151.13	$-19122x+33.157$	0.99	61.27	$-7753.1x+14.339$	0.99
	0.5	65.69	$-8311.4x+14.778$	1.00	74.86	$-9472.4x+16.207$	0.99	116.89	$-14791x+24.256$	0.98	44.27	$-5601.2x+10.55$	0.99
	0.6	55.00	$-6959.7x+12.165$	1.00	55.08	$-6969.3x+11.948$	0.98	94.90	$-12008x+18.806$	0.99	36.62	$-4633.5x+8.8083$	0.99
	0.7	50.73	$-6419.6x+10.893$	1.00	47.51	$-6011.6x+10.167$	0.96	81.66	$-10333x+15.48$	1.00	33.40	$-4226.2x+7.9628$	0.99
	0.8	49.49	$-6261.8x+10.212$	1.00	42.42	$-5367.2x+8.9817$	0.95	69.86	$-8839.1x+12.948$	0.99	31.65	$-4005x+7.4018$	0.98
	0.9	64.30	$-8136.4x+11.556$	0.87	41.97	$-5310.1x+8.5638$	0.95	61.34	$-7760.9x+11.171$	0.98	36.39	$-4604.2x+7.6357$	0.91
	Mean	66.31		0.98	84.46		0.97	98.02		0.99	48.64		0.89
Starink	0.1	42.40	$-5119x+6.2336$	1.00	47.42	$-5725x+6.9599$	0.98	24.54	$-2962.4x-1.0124$	0.90	38.74	$-4676.9x+4.5008$	0.97
	0.2	44.33	$-5351.2x+5.0607$	0.99	170.32	$-20562x+29.652$	0.90	126.09	$-15222x+19.504$	1.00	51.28	$-6190.7x+3.1272$	0.15
	0.3	126.98	$-15329x+17.552$	1.00	166.61	$-20113x+24.906$	0.99	147.05	$-17752x+21.695$	1.00	90.30	$-10901x+8.8754$	0.96
	0.4	82.75	$-9989.8x+6.6885$	0.99	105.32	$-12714x+10.65$	1.00	148.96	$-17983x+19.746$	0.99	53.96	$-6513.9x+0.7751$	0.98
	0.5	58.35	$-7044.1x+1.174$	1.00	67.72	$-8175.6x+2.5613$	0.99	112.18	$-13543x+10.68$	0.98	35.22	$-4251.3x-3.1713$	0.98
	0.6	46.34	$-5594.7x-1.5741$	1.00	45.98	$-5551.2x-1.8604$	0.96	88.18	$-10645x+5.0712$	0.99	26.30	$-3175.1x-5.0557$	0.97
	0.7	41.03	$-4953.8x-2.9757$	1.00	37.06	$-4474.2x-3.7894$	0.92	73.28	$-8846.7x+1.5891$	0.99	22.07	$-2664.3x-6.0279$	0.96
	0.8	38.88	$-4693.2x-3.7796$	1.00	30.76	$-3713.7x-5.1079$	0.90	60.04	$-7248.1x-1.0664$	0.98	19.28	$-2328x-6.7205$	0.94
	0.9	52.92	$-6388.9x-2.6285$	0.81	29.38	$-3547x-5.6427$	0.89	50.23	$-6063.5x-2.9621$	0.98	22.75	$-2746.8x-6.669$	0.77
	Mean	59.33		0.98	77.84		0.95	92.28		0.98	39.99		0.85
Vyazovkin	0.1	41.95	$-5045.3x+4.8516$	1.00	46.95	$-5646.7x+5.5659$	1.00	23.90	$-2875.1x-2.4286$	0.89	38.24	$-4599.8x+3.1097$	0.97
	0.2	43.80	$-5268x+3.6544$	0.99	170.06	$-20454x+28.194$	0.99	125.65	$-15113x+18.044$	1.00	50.57	$-6082.8x+1.669$	0.15
	0.3	126.47	$-15212x+16.076$	1.00	166.22	$-19993x+23.426$	1.00	146.61	$-17635x+20.219$	1.00	89.59	$-10775x+7.3868$	0.96
	0.4	81.98	$-9860x+5.1933$	0.99	104.61	$-12583x+9.1525$	0.99	148.46	$-17856x+18.256$	0.99	53.01	$-6376.2x-0.732$	0.98
	0.5	57.39	$-6903.3x-0.3375$	1.00	66.77	$-8031.5x+1.0451$	1.00	111.44	$-13404x+9.1716$	0.98	34.10	$-4101.3x-4.6958$	0.97
	0.6	45.25	$-5443.1x-3.1007$	1.00	44.84	$-5393.7x-3.3946$	1.00	87.24	$-10494x+3.5451$	0.96	25.05	$-3013.1x-6.5961$	0.96
	0.7	39.83	$-4790.9x-4.5167$	1.00	35.78	$-4303.4x-5.3401$	1.00	72.18	$-8681.6x+0.0457$	0.99	20.71	$-2490.8x-7.5824$	0.96
	0.8	37.57	$-4519x-5.3342$	1.00	29.35	$-3529.9x-6.6735$	1.00	58.79	$-7071.3x-2.6235$	0.98	17.81	$-2141.7x-8.2896$	0.93
	0.9	51.50	$-6194.8x-4.2045$	0.80	27.86	$-3351.1x-7.2212$	0.80	48.84	$-5874.9x-4.5324$	0.97	21.12	$-2540.4x-8.2584$	0.74
	Mean	58.42		0.97	76.94		0.97	91.46		0.98	38.91		0.85

Fig. 3 Activation energy versus mass conversion point for co-pyrolysis and co-combustion of sludge and coal

took place at α of 0.5. The average Ea of SS calculated by FWO, Starink, and Vyazovkin models as 77.90, 72.09, and 71.29 kJ mol^{-1}, respectively, was lower than that of coal. This may be due to the high volatile matter in SS [29]. The average coefficient of determination (R^2) was 0.99 for all models, indicating that the models fitted the experimental data very well.

As for SS and coal, Ea of 25SS and 50SS showed different variations. For 25SS Ea decreased for α from 0.1 to 0.2 and then increased with α except 0.8. This fluctuation may be due to the nature of molecules formed in the mixture. The increase in Ea showed that the decomposition of strong bond molecules started with increasing temperature [28]. The average Ea calculated by FWO, Starink, and Vyazovkin models of 25SS were 177.72, 176.31, and 175.85 kJ mol^{-1} and greater than that of 50SS as 170.36, 168.76, and

168.29 kJ mol^{-1}, respectively. For 50SS, Ea increased with α independently to the models used (Fig. 3). This increasing variation of Ea can be due to the progressive degradation of simple molecules to the more complex molecules in SS and coal. In fact, hydrogen is contained in biomass flocks together with coal components to form complex molecules. Since nitrogen in biomass and sulfur in coal are present, the mixture also allows the formation of bonds N–S, N–H, and H–S which are strong bonds difficult to break [30].

To investigate the synergy between SS and coal, the experimental (obtained using Starink) and calculated Ea values were compared as given in Table 5. The results showed that the deviation for Ea of 25SS obtained for α of 0.1, 0.2, and 0.8 was negative, indicating the absence of synergy. However, it was noted that overall, there was a synergy between SS and coal depending on their proportions in the

Table 5 Deviation between the experimental and calculated values of Ea during pyrolysis and combustion

Starink		Experimental Ea/kJ mol^{-1}				Calculated Ea/kJ mol^{-1}		Deviation/kJ mol^{-1}	
	α	Coal	Sludge	25SS	50SS	25SS	50SS	25SS	50SS
Pyrolysis	0.1	51.58	45.69	42.97	36.78	50.11	48.64	−7.14	−11.86
	0.2	46.81	78.82	28.50	92.35	54.82	62.82	−26.31	29.53
	0.3	36.82	88.40	118.74	127.58	49.72	62.61	69.03	64.96
	0.4	97.11	95.37	162.37	144.84	96.68	96.24	65.69	48.60
	0.5	153.88	98.40	206.07	159.24	140.01	126.14	66.06	33.10
	0.6	171.36	86.34	264.83	188.99	150.10	128.85	114.73	60.14
	0.7	158.24	71.36	318.78	220.27	136.52	114.80	182.26	105.47
	0.8	227.11	62.46	82.87	274.78	185.95	144.79	−103.08	129.99
	0.9	231.26	21.95	361.63	273.99	178.93	126.60	182.70	147.38
Average		130.47	72.09	176.31	168.76	115.87	101.28	60.44	67.48
Combustion	0.1	42.40	38.74	47.42	24.54	41.49	40.57	5.94	−16.03
	0.2	44.33	51.28	170.32	126.09	46.06	47.80	124.26	78.29
	0.3	126.98	90.30	166.61	147.05	117.81	108.64	48.80	38.41
	0.4	82.75	53.96	105.32	148.96	75.55	68.35	29.77	80.61
	0.5	58.35	35.22	67.72	112.18	52.57	46.78	15.16	65.40
	0.6	46.34	26.30	45.98	88.18	41.33	36.32	4.65	51.86
	0.7	41.03	22.07	37.06	73.28	36.29	31.55	0.77	41.73
	0.8	38.88	19.28	30.76	60.04	33.98	29.08	−3.22	30.96
	0.9	52.92	22.75	29.38	50.23	45.38	37.84	−16.00	12.39
Average		59.33	39.99	77.84	92.28	54.50	49.66	23.35	42.62

mixture. For 50SS, except α of 0.1, all deviation values were positive, showing synergy in this mixture. It can easily be seen that the average Ea of 25SS and 50SS was closer to that of coal than that of SS independently of the models used. It was also worth noting that the average Ea of blends were closer to each other compared to Ea of SS and coal. High Ea values of blends showed that the combination of SS and coal leads to the formation of more complex molecules than that contained in SS and coal themselves.

Combustion kinetic

As in pyrolysis and co-pyrolysis processes, here too Ea was a function of α. For SS and coal, Ea increased with α from 0.1 to 0.3, then decreased with α except 0.9 (Fig. 3). The average Ea values of coal calculated by FWO, Starink, and Vyazovkin were 66.31, 59.33, and 58.42 kJ mol^{-1}, respectively, and higher than that of SS determined as 48.64, 39.99, and 38.91 kJ mol^{-1}. The average Ea values of SS and coal were high compared to that reported by Li et al. [31] as 19.37 and 59.11 kJ mol^{-1}, respectively. The average Ea of SS was low when compared to that reported by Lin et al. [4] for SS as 168.94 kJ mol^{-1}. The Ea values at a low a value for may be due to the decomposition of carbohydrates and lipids whose chemical bonds have poor thermal stability [32]. Low Ea values of SS indicated that it is easier to fire than coal due to its large amount of volatile matter [29]. This difference

shows that coal contains more complex molecules than SS. It should be noted that for all samples Ea values followed the same trend regardless of the model used. However, the average Ea values calculated by Starink and Vyazovkin models were closer to each other than those calculated by FWO.

For 25SS and 50SS, the variation trends of Ea were different from that of pure SS and coal. Indeed, for 25SS, Ea increased with α between 0.1 and 0.2 then decreased, whereas for 50SS Ea increased until $\alpha = 0.4$ then decreased (Fig. 3). For 50SS, the average Ea values calculated by FWO, Starink, and Vyazovkin models were 98.02, 92.28, and 91.46 kJ mol^{-1}, respectively; and greater than that of 25SS as 84.46, 77.84, and 76.94 kJ mol^{-1}, respectively. This difference shows that 50SS requires more energy to react than 25SS. Low Ea observed at $\alpha = 0.1$ of 50SS can be justified by the vaporization and degradation of low-chemical bonds among molecules. High values of Ea observed for 25SS and 50SS show that the combination of SS and coal leads to the formation of more complex molecules than those contained in SS and coal themselves. For both mixtures, the average R^2 was greater than 0.94, showing that the models fitted the experimental data very well. From the Ea point of view, the four samples can be ranked in ascending order as SS < coal < 25SS < 50SS. This demonstrates that SS combustion occurred more easily than coal, 25SS, and 50SS.

As in co-pyrolysis, Ea values obtained using Starink model were used to calculate the deviation between the

experimental and calculated Ea for 25SS and 50SS. In general, there was a synergistic effect between SS and coal during co-combustion. The negative deviation values observed for α of 0.8 and 0.9 in 25SS showed the end of reaction, whereas for α of 0.1 in 50SS showed the beginning of reaction. It can easily be seen that the deviation decreased from α of 0.2 for the two mixtures, which confirmed the synergistic effect with regard to volatile matters. Indeed, as temperature and α increases, energy requirement for reaction decreases. During co-combustion, the presence of oxygen causes material degradation to deviate rapidly, leading to high Ea values at the beginning of reaction. Low Ea values toward the end show that, unlike co-pyrolysis, the formation of complex molecules during co-combustion is limited due to the presence of air.

Conclusions

In this study, pyrolysis and combustion of SS, coal, and their blends were investigated in order to find the most promising blend ratio for bioenergy production. TGA experiments were performed under inert and air atmospheres by using three different heating rates of 10, 20, and 40 K min^{-1}. Kinetic models of FWO, Starink, and Vyazovkin were applied on TGA data to determine Ea values. Also, the deviation between the experimental and calculated values of mass loss, residual fraction, and activation energy was calculated in order to highlight the synergistic effect between SS and coal.

In pyrolysis and combustion processes initial and final temperatures were influenced by the proportion of SS and coal in the mixture. During pyrolysis, the residual fraction (biochar) was influenced by the mixture but show little impact on mass loss in 25SS and 50SS. The increasing order of Ea of the samples in pyrolysis was SS, coal, 50SS, and 25SS. Mass loss was significantly influenced during co-combustion. The samples in the increasing order of Ea were SS, coal, 25SS, and 50SS in combustion. The sample 50SS with smaller Ea was more suitable for bioenergy production through pyrolysis compared to 25SS, whereas the opposite was valid for combustion. Overall, the smallest Ea and residual fraction of SS indicates that it was the most suitable for bioenergy production through pyrolysis and combustion.

Compliance with ethical standards

Conflict of interest It is declared that authors have no conflict of interests.

References

1. Chen GB, Chatelier S, Lin HT, Wu FH, Lin TH. A study of sewage sludge co-combustion with Australian black coal and shiitake substrate. Energies. 2019;11(12):3436.
2. Niu S, Chen M, Li Y, Song J. Co-combustion characteristics of municipal sewage sludge and bituminous coal. J Therm Anal Calorim. 2018;131(2):1821–34.
3. Adar E, Karatop B, İnce M, Bilgili MS. Comparison of methods for sustainable energy management with sewage sludge in Turkey based on SWOT-FAHP analysis. Renew Sustain Energy Rev. 2016;62:429–40.
4. Lin Y, Liao Y, Yu Z, Fang S, Ma X. The investigation of co-combustion of sewage sludge and oil shale using thermogravimetric analysis. Thermochim Acta. 2017;653:71–8.
5. Vassilev SV, Baxter D, Andersen LK, Vassileva CG, Morgan TJ. An overview of the organic and inorganic phase composition of biomass. Fuel. 2012;94:1–33.
6. Vamvuka D, Sfakiotakis S, Saxioni S. Evaluation of urban wastes as promising co-fuels for energy production—a TG/MS study. Fuel. 2015;147:170–83.
7. Xiao H, Ma X, Liu K. Co-combustion kinetics of sewage sludge with coal and coal gangue under different atmospheres. Energy Convers Manag. 2010;51(10):1976–80.
8. Xia JQ, Li HP. Co-pyrolysis charateristics study of Dianchi Lake sludge and coal. Adv Mater Res. 2014;860:518–21.
9. Xiao P, Xu L, Wang X, Chang Z. Co-pyrolysis characteristics of coal and sludge blends using thermogravimetric analysis. Environ Prog Sustain Energy. 2015;34(6):1780–9.
10. Zhang J, Chen T, Wu J, Wu J. Multi-Gaussian-DAEM-reaction model for thermal decompositions of cellulose, hemicellulose and lignin: comparison of N2 and CO2 atmosphere. Bioresour Technol. 2014;166:87–95.
11. Biagini E, Lippi F, Petarca L, Tognotti L. Devolatilization rate of biomasses and coal–biomass blends: an experimental investigation. Fuel. 2002;81(8):1041–50.
12. Otero M, Dıez C, Calvo LF, Garcıa AI, Moran A. Analysis of the co-combustion of sewage sludge and coal by TG-MS. Biomass Bioenergy. 2002;22(4):319–29.
13. Folgueras MB, Díaz RM, Xiberta J, Prieto I. Thermogravimetric analysis of the co-combustion of coal and sewage sludge. Fuel. 2003;82(15):2051–2055.
14. Ninomiya Y, Zhang L, Sakano T, Kanaoka C, Masui M. Transformation of mineral and emission of particulate matters during co-combustion of coal with sewage sludge. Fuel. 2004;83:751–64.
15. Chen J, Mu L, Cai J, Yin H, Song X, Li A. Thermal characteristics and kinetics of refining and chemicals wastewater, lignite and their blends during combustion. Energy Convers Manag. 2015;100:201–11.
16. He C, Tang C, Liu W, Dai L, Qiu R. Co-pyrolysis of sewage sludge and hydrochar with coals: Pyrolytic behaviors and kinetics analysis using TG-FTIR and a discrete distributed activation energy model. Energy Convers Manag. 2020;203:112226.
17. Ozawa T. A new method of analyzing thermogravimetric data. Bull Chem Soc Jpn. 1965;38:1881–6.
18. Doyle CD. Estimating isothermal life from thermogravimetric data. J Appl Polym Sci. 1962;6:639–42.
19. Flynn JH, Wall LA. A quick, direct method for the determination of activation energy from thermogravimetric data. J Polym Sci Part B Polym Lett. 1966;4:323–8.
20. Vyazovkin S, Wight CA. Isothermal and non-isothermal kinetics of thermally stimulated reactions of solids. Int Rev Phys Chem. 1998;17:407–33.

21. Vyazovkin S, Wight CA. Model-free and model-fitting approaches to kinetic analysis of isothermal and nonisothermal data. Thermochim Acta. 1999;340:53–68.

22. Starink MJ. A new method for the derivation of activation energies from experiments performed at constant heating rate. Thermochim Acta. 1996;288:97–104.

23. Naqvi SR, Tariq R, Hameed Z, Ali I, Naqvi M, Chen WH, Ceylan S, Rashid H, Ahmad J, Taqvi SA, Shahbaz M. Pyrolysis of high ash sewage sludge: Kinetics and thermodynamic analysis using Coats-Redfern method. Renew Energy. 2019;131:854–60.

24. Hernandez AB, Okonta F, Freeman N. Thermal decomposition of sewage sludge under N2, CO2 and air: Gas characterization and kinetic analysis. J Environ Manag. 2017;196:560–8.

25. Otero M, Calvo LF, Gil MV, García AI, Morán A. Co-combustion of different sewage sludge and coal: a non-isothermal thermogravimetric kinetic analysis. Bioresour Technol. 2008;99(14):6311–9.

26. Zhang, Y., Zhang, L., Duan, F., Jiang, X., Sun, X., Chyang. Co-combustion characteristics of sewage sludge with different rank bituminous coals under the O2/CO2 atmosphere. J Therm Anal Calorimy. 2015;121(2):729–736.

27. Qu X, Zhou G, Cao Y, Li P, He Y, Zhang J. Synergetic effect on the combustion of lignite blended with humus: Thermochemical characterization and kinetics. Appl Therm Eng. 2019;152:137–46.

28. Merdun H, Laougé ZB. Kinetic and thermodynamic analyses during co-pyrolysis of greenhouse wastes and coal by TGA. Renew Energy. 2021;163:453–64.

29. Li H, Li Y, Jin Y. Co-combustion analyses of coal and sewage sludge with high moisture content. Energy Sour Part A Recov Util Environ Eff. 2015;37(17):1896–903.

30. Tahir MH, Zhao Z, Ren J, Rasool T, Naqvi SR. Thermo-kinetics and gaseous product analysis of banana peel pyrolysis for its bioenergy potential. Biomass Bioenergy. 2019;2019(122):193–201.

31. Li H, Li YY, Jin YY. Analyses of coal and sewage sludge co-combustion using Coats-Redfern model. Adv Mater Res. 2012;518:3271–4.

32. Cai H, Liu J, Kuo J, Buyukada M, Evrendilek F. Thermal characteristics, kinetics, gas emissions and thermodynamic simulations of (co-) combustions of textile dyeing sludge and waste tea. J Clean Prod. 2019;239:118113.

Publisher's Note Springer Nature remains neutral with regard to jurisdictional claims in published maps and institutional affiliations.